Proceedings of the 4th World Congress on Civil, Structural, and Environmental Engineering (CSEE'19)
Rome, Italy – April, 2019
Paper No. ICGRE 140
DOI: 10.11159/icgre19.140

A Comparison Study: Estimating the Axial Micropiles Capacity Using Current Practices

Ahmed Elgamal[1]
[1]Mansoura Higher Institute of Engineering and Technology
Mansoura Damietta Road, Mansoura, Egypt
Aelgamal@mc.edu.eg

Abstract **-** According to the innovation of new techniques used in building constructions, a new structural case of loading appears. An additional usage of micropiles beside the conventional purpose is needed to cope with these cases of loading. Nowadays, retrofit buildings to resist static and dynamic construction loadings is an urgent need. Due to the uneconomic of conventional piles or the restricted construction of retrofitting buildings, or to reinforce the weak soils, micropiles are appropriate to be used. Although, up to now, there is no accurate estimation of the axial capacities of micropiles (i.e., compression and tension). Current design guidelines try to introduce safe and economic methods of estimating the axial capacities of micropiles. All these guidelines recommend just preliminary designs and performing a full-scale test is a must to validate the designed capacity. A comparison study is presented in this paper to catch on the most suitable method should be used to estimate the axial micropile capacities by comparing the results to full-scale tests results. The end bearing can be neglected in the micropile design in case of the need to limit the building settlement. Some engineering design standards can be applied to design micropiles and more investigation is needed to enhance the tensile geotechnical capacity of micropiles.

Keywords**:** Micropile, Axial Capacity, Finite Element, Modelling, Design

1. Introduction

Micropiles are defined as small diameter drilled-grouted piles (e.g., 70 to 300 mm) with length to diameter ratio over 30 [1]. The micropiles can be classified according to the philosophy of behavior (the design concept) into cases 1 and 2, and according to the method of grouting (the construction concept) into types A, B, C, and D [2] as presented in Table 1. Case 1 indicates that the micropile is used as a conventional pile. Case 2 refers to the usage of the micropile to reinforce the soil. According to [3], the micropiles are not designed individually to support the structure loads but rather to reinforce the soil underneath the structure like the root system of a tree. So, the reinforced soil and the root/micro piles behave as an integrated block to resist the applied loads.

Table 1: Micropile classification based on grouting type (after [2]).

Grouting Type	Description	Grout
A	Gravity grout only	Sand/cement mortar or neat cement.
B	Pressured grout through the casing	Neat cement.
C	Primary grout placed under gravity head then pressure grouted	Neat cement.
D	Primary grout placed under gravity then repeatable post-grout	Neat cement.

The micropile axial capacity preliminary design consists of two basic aspects; 1) geotechnical design, and 2) structural design. The geotechnical design requires the ground/grout interface parameters and the initial stress state in the ground after micropile installation. The skin and the end bearing resistances govern the axial geotechnical capacity of the micropiles. However, the end bearing can be neglected in all types of soils except that rested on rocks [4]. Moreover, the composite section (i.e., the rod and the grout cross-sectional area) governs the internal structural capacity. The applied loads on the micropile head are transferred to the ground through the grout to ground skin friction with no contribution of the end resistance as suggested for the design purposes by [2].

The micropiles can be used to improve the soil behavior as introduced by [5]. A group of 100 mm diameter micropiles, 4 m length, and 20˚ inclination angle from the vertical position is used to increase the bearing capacity of the soil underneath an existing foundation. The confining micropiles technique can be used to improve the bearing capacity of loose sandy soils, especially, in the coastal areas where the higher levels of groundwater [6]. According to the same research, the bearing capacity of the sandy soil beneath the isolated footing increased to 2.28 times that of without micro-piling with spacings 2.67 times the micropile diameter. The micropile technique is a successful tool in cases of retrofit existing defective structures and constructs new buildings ([7], [9], and [10]).

This paper presents the methods recommended by the design guidelines to estimate the capacity of the micropiles subjected to axial loads in sandy and clayey soils. Comparisons between the list of micropiles design standards are presented besides numerical investigations which were calibrated using full-scale load tests.

2. Estimate the Micropile Axial Capacity

Micropiles are used to resist types of loadings (e.g., axial compression, tension, lateral, or combined between any of them with bending moments). As mentioned in the previous section, the axial performance of the micropiles is governed by the ground conditions (i.e., side friction and end bearing) which limited by the structural capacity of the micropile cross-section as illustrated in section 2.2. Figure 1 presents the typical details of a micropile.

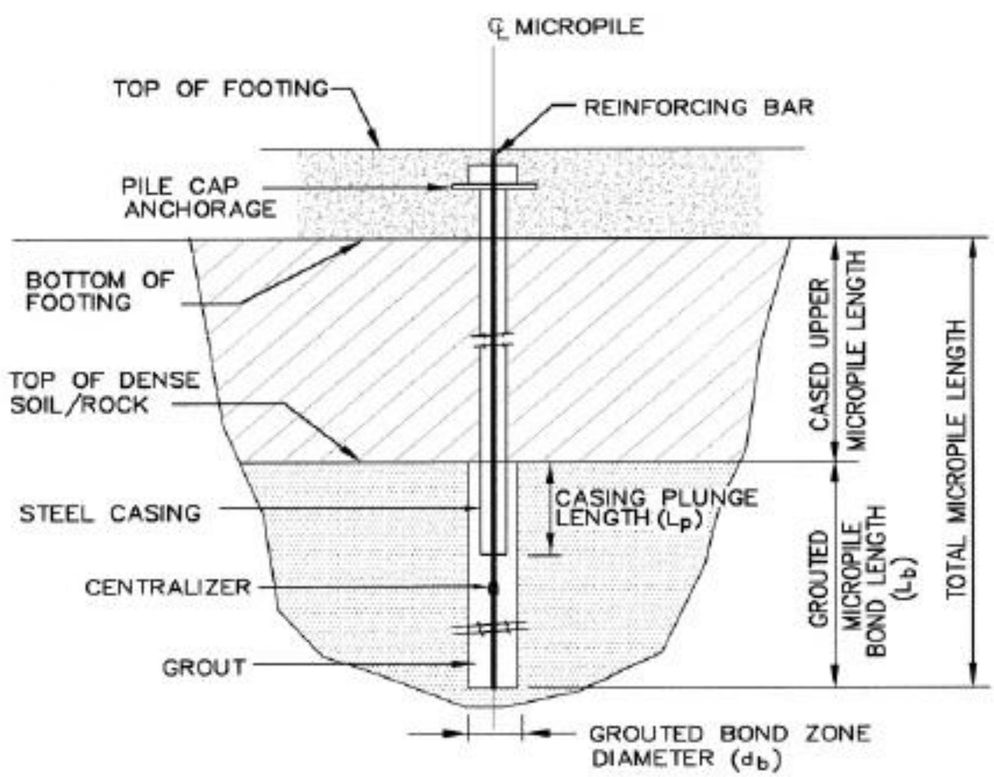

Fig. 1: Typical details of micropile (after [2]).

2.1. Structural Design

The structural capacity of micropiles is controlled by the nature of the pile cross-section. Figure 1 presents a typical cross-section of reinforced-cased micropile. Using the mono reinforcing bar, multiple bars, rolled steel, or a casing of steel steel pipe to reinforce the micropile are suggested by [2]. The main advantages of these reinforcements are to increase the the axial capacity and resist the bending moment produced from the lateral load at the pile head or from the pile buckling. Also, the grouting material has a significant effect on the axial compression capacity. Table 2 shows the different methods recommended by design guidelines to estimate the compression (P_{Sc}) and tension (P_{St}) capacities of micropiles.

Table 2: Structural Capacities of micropiles using design standards.

Method	Axial structural capacities
FHWA (2005) [2]	***Compression (ASD)*** $P_{Sc} = 0.4\ \mathrm{P}_{Grout} + 0.47\ \mathrm{P}_{Rft}$ (1a) ***Tension (ASD)*** $P_{St} = 0.55\ \mathrm{P}_{Rft}$ (1b)
DFI/ADSC (2004) [10] **IBC (2006) [11]**	***Compression (ASD)*** $P_{Sc} = 0.33\ \mathrm{P}_{Grout} + 0.4\ \mathrm{P}_{Rft}$ (2a) ***Tension (ASD)*** $P_{St} = 0.6\ \mathrm{P}_{Rft}$ (2b)
BS-8110	***Compression (ASD)*** $P_{Sc} = 0.4\ \mathrm{P}_{Grout} + 0.75\ \mathrm{P}_{Rft}$ (3a) ***Tension (ASD)*** $P_{St} = 0.58\ \mathrm{P}_{Rft}$ (3b)
AASHTO (2014) [12]	***Compression (LRFD)*** $P_{u,\ Sc} = 0.54\ \mathrm{P}_{Grout} + 0.637\ \mathrm{P}_{Rft}$ (4a) ***Tension (LRFD)*** $P_{St} = 0.8\ \mathrm{P}_{Rft}$ (4b)

$\mathrm{P}_{Grout} = f_c^{'}\ A_{grout}$; $\mathrm{P}_{Rft} = f_{y-bar}\ A_{bar} + f_{y-casing}\ A_{casing}$

ASD = Allowable Stress Design; LRFD = Load Resistance Factor Design

Where, $f_c^{'}$ is the unconfined compressive strength of the grout, A_{grout} is the cross-sectional area of the grout, f_{y-bar} and $f_{y-casing}$ are the yield strengths of the steel bar and casing, respectively, and A_{bar} and A_{casing} are the cross-sectional areas of reinforcement and cased pipe, respectively.

The Allowable Stress Design (ASD) method tends to use a constant factor of safety (FS) to the ultimate capacity of the piles. This FS is constant regardless of the material used or the nature of the applied load. The Load and Resistance Factor Design (LRFD) technique started to be applied to the design of substructures (e.g., micropiles) by [12]. The LRFD procedure applies variable factors of safety considering the structural material (i.e., resistance factor) and the type of loading (i.e., load factor) to relate the applied load to the required resistance. The main aim of LRFD is to link the material strength to the structure serviceability using probability and statistics concepts. The LRFD design concept has been slower to catch on in geotechnical engineering. Where the traditional geotechnical engineering has been based on FS against service loads. It should be noted that the load and resistance factors compensate the FS in ASD.

2.2. Geotechnical Design

Indeed, not all the design standards have recommendations for the geotechnical design of micropiles. The β and methods are listed by [13] to estimate the preliminary design of micropiles in sandy and clayey soils, respectively. The of α and β influenced by the grout-ground interaction and the grouting type (see Table 3). As introduced before, the capacity of micropiles can be covered by the side resistance using methods shown in Table 3.

Equation 5 is recommended by [2] to calculate the allowable geotechnical capacity of micropiles (PG) using the ultimate grout-ground bond resistance (α_bond) which can be calculated using Table 4. The side resistance mobilized through the bond length of the micropile cab be calculating as:

$$P_G = \frac{\alpha_{bond}}{FS}\,\pi\, D_b\, L_b \tag{5}$$

Where, D_b is the diameter of the pile, and L_b is the bond length. The factor of safety (FS) is recommended to be 2.5 [2].

The axial compression capacity is increased by adding the tip resistance in the case of resting on the rock [12]. AASHTO applied the LRFD grout-ground bond resistance factor to the pile skin friction as obtained from the following equation. The values of α_{bond} are the same of FHWA ones shown in Table 4.

$$P_{u,GC} = 0.55\,\alpha_{bond}\,\pi\, D_b\, L_b \tag{6}$$

Table 3: Preliminary design of micropiles (after [13]).

Soil Type	Micropile Type					
	Type A		Type B		Type C	Type D
Sand	β method	$P_{Gc} = \beta\,\sigma_{vo}\,A_s$ Where, $\beta = 0.7 \tan\varphi$		$P_{Gc} = \beta\,\sigma_{vo}\,A_s$ Where, $\beta = K_1 K_2 \tan\varphi$, $K_1 = 1.4$ to 1.7, $K_2 = 1.2 : 1.5$, dense $= 1.5 : 2.0$, Medium	Use typical Charts presented by [14]	
Clay	α method	$P_{Gc} = \alpha\,S_u\,A_s$ Where $\alpha = 0.6$ to 0.8			Use typical Charts presented by [15]	

σ_{vo} = vertical effective stress; A_s = pile side area; φ = soil friction angle; S_u = soil undrained shear strength

Table 4: Typical values of ultimate grout-ground bond strength (after [2]).

Soil	Ultimate Grout-Ground bond strength α_{bond} (kPa)			
	Type A	**Type B**	**Type C**	**Type D**
Medium Silt / Soft Clay	35-70	35-95	50-120	50-145
Dense Silt / Stiff Clay	50-120	70-190	95-190	95-190
Fine, Loose, Medium Sand	70-145	70-190	95-190	95-240
Fine-Coarse, Medium-very dense Sand	95-215	120-360	145-360	145-385

The end bearing of micropiles is recommended to be neglected by all design guidelines except when the micropile rests on a rock. This recommendation is because of the large displacement needed to fully mobilize the end bearing (6% of pile diameter, [12] or about 20 to 40 times less than those required for the end bearing [13]). The side resistance is mobilized after reaching a micropile displacement of about 2.5 to 10 mm [12]. Using the same methods of drilled shafts to calculate the end bearing of micropile as in the following equation are suggested by [2].

$$P_{u,GC} = N_q \sigma_{vo} A_s \tag{7}$$

Where Nq is a bearing load factor ranges between 50 to 100 for bored piles in dense sandy soils, and σ_vo is the vertical effective stress at the pile tip.

3. Case Study

Two full-scale pile load tests are used to measure the accuracy of the current practice approaches used to estimate the micropile axial compressive and tensile capacities. Beside numerical investigations using a Finite Element (FE) program (i.e., MIDAS GTS NX).

3.1. Italian Alpine Region Full-scale test

A series of full-scale axial compression and tensile load tests were performed by [16], in Italian Alpine Region, on Type A micropiles with 200mm in diameter. A mixture of silt with sand and gravel is extended to 9 m depth below the ground surface which discontinued at a depth of 6m by the 2.0 m thick of mixture of gravel with silt and sand. No water table was detected at the testing site. The soil and micropile properties are presented in Tables 5 and 6, respectively.

Table 5: Soil properties of the case study (after [16]).

Soil depth (m)	**Soil type**	**Unit weight γ, kN/m^3**	**Friction angle φ, degree**	**Undrained compressive strength S_u, kPa**
0.0 – 6.0	Sandy silt with some gravel	17.0	25˚	100 - 110
6.0 – 8.0	Sandy gravel with a trace of silt	19.0	42˚	-
8.0 – 9.0	Sandy silt with gravel	19.0	42˚	-

Table 6: Micropile properties of the case study (after [16]).

No.	**Load Type**	**Total Length (m)**	**Embedded Length (m)**	**Hole Dia. (mm)**	**Casing**		**Bar RFT Dia. (mm)**	**Grout Type**
					Outer Dia. (mm)	**Thickness (mm)**		
1	C	7.05	6.65	200	127	10	32	A
2	T	6.89	6.54	200	127	10	32	A

C = Compression; T = Tension

3.2. Finite Element Model (FEM)

Figure 2 portrays the general layout dimensions of the FEM. MIDAS GTS NX is used to generate the three-dimensional soil-pile model. A pile with total length (L) and diameter (D) is embedded into the soil profile shown in Table 5. The hybrid mesh size is extended to 16D from the center of the pile to release the effect of boundary conditions. The model is restrained at the bottom face, and the vertical sides are fully fixed in X- and Y- directions.

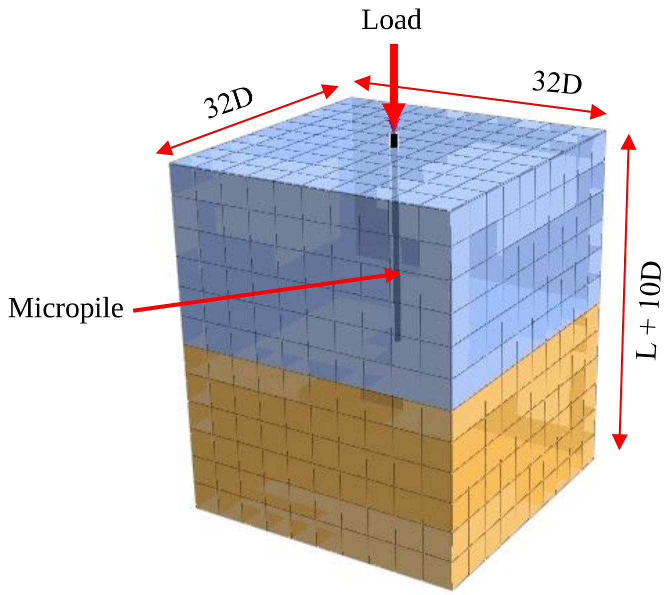

Fig. 2: The layout of the FE model.

The Mohr-Coulomb criteria are applied to model the soil, and a linear-elastic material is used for the micropile. The soil and pile properties used in the FE modeling are presented in Tables 7 and 8, respectively. The soil-pile interface in MIDAS can be produced using: 1) the ultimate shear force (Q_u) which represents the ultimate skin friction that can be calculated using design standards (e.g., [2]), 2) the shear stiffness modulus (K_t) which is a function of soil shear modulus (G) using soil modulus of elasticity (E) and soil Poisson`s ratio (ν) as in Eq. 7, and 3) the normal stiffness ($K_n$) using the interface Poisson`s ration (ν_{int}) as in Eq. 8. It should be noted that the values of Q_u, K_t, and K_n are calculated per the pile total length.

$$K_t = \frac{G}{L\, t_v}, \text{ where } G = R\, \frac{E}{2\,(1+\nu)} \tag{7}$$

$$K_n = \frac{E_{oed}}{L\, t_v}, \text{ where } E_{oed} = 2\, G\, \frac{(1-\nu_{int})}{2\,(1-2\,\nu_{int})} \tag{8}$$

According to MIDAS user manual [17], R is a reduction factor for interface strength which ranges from 0.6 to 0.7 and 0.8 to 1 for steel and concrete piles, respectively, t_v is a virtual thickness for the interface element that has a value between 0.01 to 0.1.

Table 7: Sand Properties Used in FEM.

Depth	**γ(kN/m^3)**	**φ (degree)**	**S_u (kPa)**	**ν***	**E* (kN/m^2)**
0.0 – 6.0	17	25	105	0.30	25000
6.0 – 9.0	19	42	-	0.35	40000

* Values of soil Poisson`s ratio (ν) and modulus of elasticity (E) are assumed according to Bowles (1996).

Table 8: Piles Properties Used in FEM.

Section	**D (mm)**	**L (m)**	**EI ($kN\text{-}m^2$)**	**Interface Parameters**			
				Depth (m)	Q_u (kN/m^2)	K_t (kN/m^3)	K_n (kN/m^3)
Circular	200	7.05	2383.6	0.0 – 6.0	95	112179.5	1233974
				6.0 – 9.0	95	1656805	18224852

3.3. Analysis and Results

Figure 3 presents the load-displacement curves of the compression and tensile tests from the full-scale test reported by [16] and the one calculated using FEM. Despite the good agreement observed in Fig. 3, the FE model is sensitive to the interface element parameters especially the value of t_v ([18]; [19]). As portrayed in Fig. 3a, the end bearing has a significant effect on the axial response of micropiles. However, the design guidelines recommend using only the shaft resistance due to the limitation of micropile displacements.

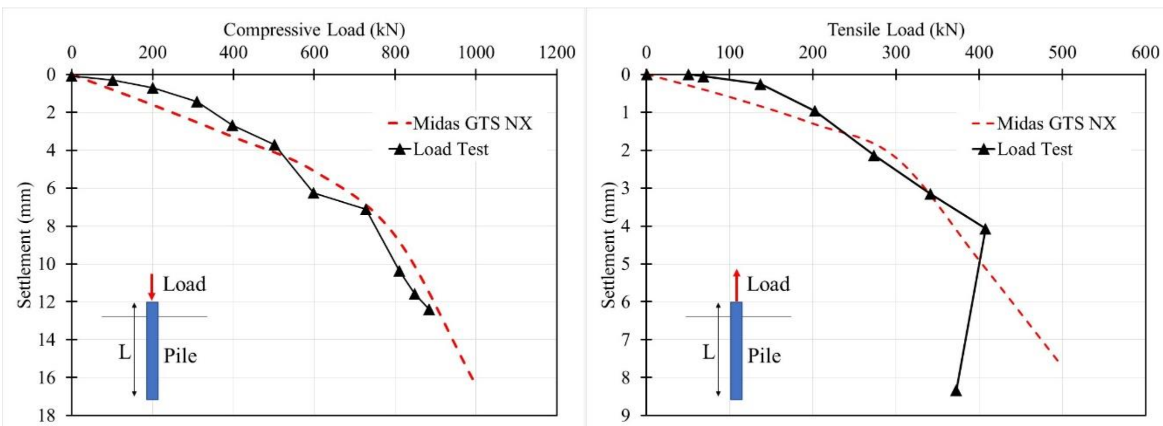

(a) Compression full-scale test (Test C) (b) Tensile test (Test T)

Fig. 3: Load-displacement tests for compressive and tensile loads.

The ultimate compressive capacity has been determined from the full-scale test and FEM results using [20] method as shown in Table 9. The estimated ultimate capacities, using previously mentioned design guidelines, are compared to those obtained from the full-scale tests and FEM results (see Table 9 and Fig. 4). When considering that the axial capacity, the results obtained from [10] and BS-8110 are the nearest to the full-scale tests. But for considering both the geotechnical and structural capacities, [2] and [12] are the most applicable methods.

Table 9: Axial capacities of Italian Alpine Region test.

Method	$P_{G,all}$ (kN)		$P_{S,all}$ (kN)		P_{all} (kN)	
	Side	**Tip**	**Comp.**	**Tension**	**Comp.**	**Tension**
Full-Scale using [20]	P_u = 830 kN in **compression**, P_{all} = 332 kN (FS = 2.5)					
	P_u = 375 kN in **tension**, P_{all} = 133 kN (FS = 2.5)					
FE model using [20]	P_u = 890 kN in **compression**, P_{all} = 356 kN (FS = 2.5)					
	P_u = 520 kN in **tension**, P_{all} = 208 kN (FS = 2.5)					
FHWA (2005) [2]	184	111	360	590	295	184
DFI and ADSC (2004) [10]	N/A	N/A	360	650	360	184
BS-8110	N/A	N/A	360	630	360	184
AASHTO (2014) [12]	180	111	360	870	291	180
JURAN et al. (1999) [13]	70	111	N/A	N/A	181	70

FS = 1.4 is applied to the AASHTO results
The structural tension capacity is used equally to FHWA (2005) for N/A values

Figure 4 presents the ratio between the calculated to the full-scale axial capacities for Italian Alpine Region micropiles. It should be noted that the allowable axial compression capacities shown in Table 9 are calculated by adding the skin resistance to the end bearing of the micropile as derived by [16]. Also, the allowable structural capacity is limited by the axial compression force which causes the pile buckling. Moreover, the uplift capacity of micropiles needs to be reduced using a multiplier of 0.72 to match the estimated capacity to the measured one.

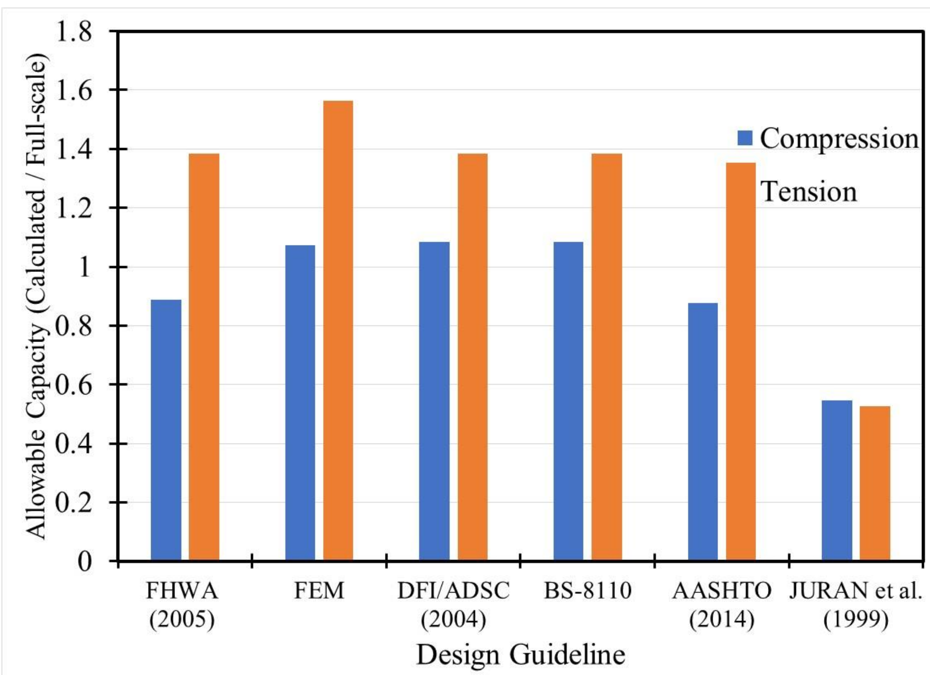

Fig. 4: Load-displacement tests for compressive and tensile loads.

4. Conclusion

The allowable compression and tension capacities of micropiles are investigated using Finite Element models and the results are compared to those obtained from a full-scale test performed at the Italian Alpine Region. Also, the micropile capacities are estimated using current practices (i.e., FHWA, AASHTO, DFI/ADSC, BS, and α-β methods). Through this study the following results are founded:

1. The FHWA (2005) and AASHTO (2014) design guidelines are the most accurate methods to calculate the axial compression capacity of micropiles.
2. The axial tensile capacity of micropile needs more investigation to reduce the estimated values obtained using current practices. The current study recommends a multiplier equal to 0.72.
3. In case of limited structure settlements, the design of micropiles should only consider the side resistance and the end bearing can be neglected.
4. In case of using of micropiles as an alternative solution comparing to the traditional drilled shafts, no need to depend only on the side resistance but also the end bearing should be added to minimize the construction cost.
5. A sensitivity analysis should be performed on the interface element parameters in FE programs to determine formulas consider micropiles especially the grouting type.

References

[1] D. Liu, J. Zheng, and L. Liu, "Current Situation Review of the Micropile," *Int. J. Comput. Eng.*, vol. 1, no. 1, pp. 81-86, 2016.

[2] FHWA, "Micropile Design and Construction Guidelines," *Handbook*, no. NHI 132078, p. 456, 2005.

[3] F. Lizzi, "Reticulated root piles to correct landslides," *ASCE Conv.*, p. Preprint 3370, 1978.

[4] A. Cadden, J. Gomez, D. Bruce, and T. Armour, "Current Practices and Future Trends in Deep Foundations," in *Current Practices and Future Trends in Deep Foundations*, 2004, pp. 140-165.

[5] Y. D. Honrao, A. Gupta, and D. Desai, "Micro - piles," *IOSR J. Mech. Civ. Eng.* , pp. 48-50, 2009.

[6] N. Unnikrishnan and P. Sachin, "Influence of Confining Micro Piles on the Bearing Capacity of Sand," in I*NTERNATIONAL FOUNDATION CONGRESS AND EQUIPMENT EXPO*, 2009, pp. 367-374.

[7] P. D. Martin, "Micropile foundations for ESSROC cement plant expansion," *Contemporary Topics in Deep Foundations - 2009 International Foundation Congress and Equipment Expo*. pp. 375-382, 2009.

[8] B. Byford and M. Hampton, "Micropiles for re-support and lifting of two buildings under construction," *Geotechnical Special Publication*, no. 185. pp. 383-389, 2009.

[9] J. B. Pease, *Use of Multiple Techniques to Support Construction of a New Hospital Addition*. 2009.

[10] DFI and ADSC, *GUIDE TO DRAFTING A SPECIFICATION FOR MICROPILES*. Hawthorne, New Jersey and Dallas, Texas, 2004.

[11] IBC, *International Building Code*. 2006.

[12] (American Association of State Highway and Transportation Officials) AASHTO, *AASHTO LRFD Bridge Design Specification*, 7th ed. 2014.

[13] I. Juran, D. A. Bruce, A. Dimilliot, and A. Benslimane, "Micropiles: the state of practice. Part II: design of single micropiles and groups and networks of micropiles," *Gr. Improv.*, vol. 3, pp. 89-110, 1999.

[14] H. Ostermayer and F. Scheele, "RESEARCH ON GROUND ANCHORS IN NON-COHESIVE SOILS," *revenue française de géotechnique*, vol. 3, pp. 92-97, 1978.

[15] H. Ostermayer, "Construction, carrying behavior and creep characteristics of ground anchors," in *DIAPHRAGM WALLS & ANCHORAGES*, 1975, pp. 141-151.

[16] D. Bellato, S. D'Agostini, and P. Simonini, "Interpretation of failure load tests on micropiles in heterogeneous Alpine soils," *Ital. Geotech.*, vol. 47, no. 1, pp. 3-16, 2013.

[17] MIDAS User Manual, "Midas Users Manual." 2014.

[18] M. Ashour, A. AlaaEldin, and M. G. Arab, "Battered Piles under Lateral Loads using Strain Wedge Model and Current Practice Mohamed," *New York Sci. J.*, vol. 11, no. 7, pp. 20-28, 2018.

[19] Y. H. Ong, “Back analysis of laterally loaded pile behavior using Midas/GTS to determine stiffness modulus of pile-soil interface,” *Japanese Geotech. Soc. Spec. Publ.*, vol. 2, no. 35, pp. 1279-1284, 2015.

[20] M. T. Davisson, “High capacity piles,” in *Proceedings, Lecture Series, Innovations in Foundation Construction, ASCE*, 1972, p. 52.